1. Title page

Cardiovascular molecular imaging with fluorine-19 MRI – the road to the clinic

Authors: Ruud B. van Heeswijk, PhD[1]*; Wolfgang Bauer, MD[2]; Florian Bönner, MD[3]; Jelena M. Janjic, PhD[4]; Willem J.M. Mulder, PhD[5,6]; Laura M. Schreiber, PhD[7]; Juerg Schwitter, MD[8,9.10]; Ulrich Flögel, PhD[11,12]

Affiliations:

1. Department of Radiology, Lausanne University Hospital (CHUV) and University of Lausanne (UNIL), Lausanne, Switzerland.

2. Department of Internal Medicine I, Universitätsklinikum Würzburg, Würzburg, Germany.

3. Department of Cardiology, Pulmonology, and Vascular Medicine, Medical Faculty of Heinrich Heine University, University Hospital Düsseldorf, Germany

4. Graduate School of Pharmaceutical Sciences, School of Pharmacy, Duquesne University, Pittsburgh, PA, USA

5. Laboratory of Chemical Biology, Department of Biochemical Engineering,

Eindhoven University of Technology, Eindhoven, The Netherlands

6. Department of Internal Medicine and Radboud Center for Infectious Diseases,

Radboud University Medical Center, Nijmegen, the Netherlands

7. Chair of Molecular and Cellular Imaging, Comprehensive Heart Failure Center (CHFC), Wuerzburg University Hospitals, Wuerzburg, Germany

8. Division of Cardiology, Cardiovascular Department, Lausanne University Hospital (CHUV), Lausanne, Switzerland

9. CMR Center, Lausanne University Hospital (CHUV), Lausanne, Switzerland

10. Faculty of Biology and Medicine, University of Lausanne (UNIL), Lausanne, Switzerland

11. Experimental Cardiovascular Imaging, Heinrich Heine University, Düsseldorf, Germany

12. Cardiovascular Research Institute Düsseldorf (CARID), Heinrich Heine University, Düsseldorf, Germany

Short title: A review of cardiovascular fluorine-19 MRI

Journal Subject Terms: Magnetic Resonance Imaging, Inflammation, Thrombosis, Animal Models of Human Disease, Translational Studies

*Corresponding author:
Ruud van Heeswijk, PhD
ruud.mri@gmail.com
Lausanne University Hospital (CHUV)
Department of Radiology
Rue de Bugnon 46, BH08.084
1011 Lausanne, Switzerland
tel. +41-21-3147535
orcid.org/0000-0001-5028-4521

Word count: 5973 of 6000

2. Abstract (unstructured, 150w)

Fluorine-19 magnetic resonance imaging (^{19}F MRI) is a unique quantitative molecular imaging modality that makes use of an injectable fluorine-containing tracer that generates the only visible ^{19}F signal in the body. This "hot spot" imaging technique has recently been used to characterize a wide array of cardiovascular diseases and seen a broad range of technical improvements. Concurrently, its potential to be translated to the clinical setting is being explored. This review provides an overview of this emerging field and demonstrates its diagnostic potential, which shows promise for clinical translation. We will describe ^{19}F MRI hardware, pulse sequences, and tracers, followed by an overview of cardiovascular applications. Finally, the challenges on the road to clinical translation are discussed.

3. Keywords (3-6)

Cardiovascular

Fluorine-19

Magnetic resonance imaging

Inflammation

Cell tracking

Molecular imaging

4. Abbreviations List

AMI – acute myocardial infarction

CAD – coronary artery disease

COPD – chronic obstructive pulmonary disease

^{18}FDG-PET – fluorodeoxyglucose-18 positron emission tomography

^{19}F – fluorine-19

^{1}H – hydrogen

LGE – Late gadolinium enhancement

LoD – Limit of detection

MRI – magnetic resonance imaging

PAD – peripheral artery disease

PE – pulmonary embolism

PFC – perfluorocarbon

PFCE – perfluoro-15-crown-5-ether

PLGA – poly(lactic-co-glycolic acid)

PFOB – perfluoro-octylbromide

PFTBH – perfluoro-tert-butylcyclohexane

RF – radiofrequency

SNR – signal-to-noise ratio

WBC-SPECT – white blood cell single-photon emission computed tomography

5. Introduction

While magnetic resonance imaging (MRI) is primarily known for its ability to anatomically visualize soft tissues, fluorine-19 MRI (^{19}F MRI) is a unique molecular imaging modality that makes use of an injectable fluorinated tracer and dedicated hardware. As the tracer generates the only detectable ^{19}F signal in the body, its accumulation can be quantitatively and longitudinally visualized as "hot spots" (Figure 1). Compared to other cardiovascular molecular imaging modalities, the main advantages of ^{19}F MRI are the absence of ionizing radiation, easy coregistration with anatomical MRI, and a relatively high spatial resolution (Table 1).

Propelled by technical advances, ^{19}F MR hot spot imaging has recently been developed into an *in vivo* modality to characterize a wide array of pathological processes in cardiovascular disease models. With the first clinical study expected soon, an overview of the principles of ^{19}F MRI and its applications to cardiovascular disease is warranted. The goal of this review is to both provide an overview of advances in the ^{19}F MRI field and to elaborate on its clinical diagnostic potential. We will set out the medical need, describe the hardware and pulse sequences, provide insight in ^{19}F MRI tracers, which are predominantly based on perfluorocarbons (PFC), and highlight its application for cardiovascular inflammation imaging. Finally, we will discuss the remaining hurdles on the road to clinical translation.

Medical needs

Today, conventional MRI is a valuable modality for the diagnosis and stratification of cardiovascular inflammation: it for example allows visualizing edema using T_2 mapping and necrosis/fibrosis using late gadolinium enhancement (LGE). However, beyond these measures, conventional MRI is somewhat limited for molecular imaging approaches. In order to create

contrast, (cellular) targets of interest have to be tagged with (super)paramagnetic agents.[1] Despite its excellent sensitivity, this has the disadvantage that those agents create hypo/hyperintense spots with the entire anatomy of the investigated region as background signal, which makes unambiguous identification *in vivo* difficult or even impossible. Here, positron emission tomography (PET) approaches in combination with computed tomography or MRI offer superior specificity, although conventional fluorodeoxyglucose-18 (^{18}FDG) PET requires suppression of myocardial glucose metabolism to make that of inflammatory cells visible. Alternatively, ^{68}Ga-labeled probes can be used to specifically target for example the innate immune system (CXCR4[2,3] and CCR2[4]) or proinflammatory macrophages.[5] However, the drawbacks of PET are its low spatial resolution, the exposure to ionizing radiation, and the relatively short half-life of the used tracers, which requires on-time synthesis in a cyclotron and precludes their monitoring over longer periods of time such as several days. Similar to PET, ^{19}F MRI is also a background-free modality, but relies on the stable isotope ^{19}F to overcome several of the issues outlined above (Table 1). Since ^{19}F MRI has been proven in experimental models to be applicable for the sensitive detection of inflammatory patterns, distinct stages of thrombosis and specific cell populations, it may facilitate clinical decision making in a variety of settings.[6–8]

Inflammation and cell tracking: The non-invasive identification of distinct inflammatory processes without the need for endomyocardial biopsies (EMBs) could help guide disease management in myocarditis, which is a common disease and its prevalence trends to increase not only due to Covid-19,[9] but also due to modern anti-cancer treatments.[10] Similar considerations apply to non-humoral heart transplant rejection, which continues to be a significant threat in the surveillance of patients after transplantation. Currently, EMB is conducted serially to early diagnose transplant rejection, regardless of symptoms. Clearly, EMB is an important patient

stressor and prone to sampling errors. Thus, alternatives to invasive testing and unspecific imaging approaches are urgently needed. Important applications are also conceivable in the context of acute myocardial infarction (AMI) and the underlying cause of many cardiovascular diseases, atherosclerosis. Since ^{19}F MRI holds the potential to characterize the role of distinct leukocyte populations, it could yield spatial information on the contribution of different immune cell subsets to reperfusion injury in the directly affected myocardium and along the infarct border zone. Using (multi)-targeted approaches,[11] even bone marrow activation and the entire development cascade from atherosclerosis to AMI[12] can be tracked. Immune-cell-specific ^{19}F MRI approaches further harbor the potential for identification and treatment guidance[13] of patients with stable coronary artery disease, but plaque-derived inflammation,[14] which are at risk of future complications (AMI, stroke).

Thrombosis: The diagnosis of acute pulmonary embolism (PE), the third leading cause of cardiovascular mortality, with fibrin-targeted ^{19}F MRI has also shown potential in an experimental model.[15] While prompt diagnosis is potentially lifesaving, currently various multi-step algorithms are applied in clinical routine to decide to proceed to an imaging test. CT pulmonary angiography is widely used because of its high sensitivity and specificity, but it comes with radiation exposure that is undesirable, particularly in younger female patients, and the analysis based on the identification of filling defects in pulmonary arteries is time-consuming. Here, ^{19}F MRI represents an elegant method to highlight thrombi as hot spots without background signals, thereby facilitating the detection of thrombi with unmet specificity.[15]

Importantly, both inflammation and epitope-targeted ^{19}F MRI could open a large spectrum of applications beyond the cardiovascular system, for example in patients with fever of unknown

7

origin or chronic inflammatory diseases (rheumatisms, diabetes, multiple sclerosis, etc.), as in principle, any epitope can be targeted.

6. Technical aspects

Physics and hardware requirements

While conventional MRI takes advantage of the high ^{1}H abundance in water and fat in our bodies, ^{19}F MRI directly visualizes an exogenously administered fluorinated tracer. In the absence of endogenous ^{19}F signal, this type of MRI does not suffer from background signal. As ^{19}F is a stable nucleus that has a favorable spin ½ nucleus with a gyromagnetic ratio of 40.05 MHz/T, merely 5.9% smaller than that of ^{1}H, relatively low amounts of ^{19}F-based tracers can be detected.

To measure at the ^{19}F frequency, an MRI scanner needs to be equipped with a radiofrequency system that is able to transmit and receive at the Larmor frequency of the nucleus (e.g. 120MHz at 3T instead of 128MHz for routine ^{1}H MRI). While this is feasible in most small-animal scanners, clinical systems will typically need a radiofrequency amplifier upgrade for X-nuclear imaging, which is usually available for high-end clinical MRI scanners.

Moreover, dedicated radiofrequency coils are needed for radiofrequency transmission and reception. While for small-animal scanners these coils can typically be obtained from the vendor, ^{19}F coils for use in clinical MRI scanners need to be custom-built by third-party vendors. The construction of two resonant circuits in a single housing is fairly straightforward with active detuning elements, but does come at the relative cost increase of those two circuits. To allow anatomical co-registration of the ^{19}F signal, double-resonant ^{1}H/^{19}F coils are helpful to concurrently acquire the anatomical ^{1}H image.[16]

At a number of sites, ^{19}F MRI is already performed on clinical systems, both in small and large animals.[8,17] Clinical MRI scanners may be operated outside their original specifications in those cases, although the routine safety parameters of tissue heating from RF pulse energy deposition and peripheral nerve stimulation through rapidly changing magnetic field gradients cannot be overruled, guaranteeing patient safety.

Tracer formulation

[19]F MRI is commonly performed with tracers that contain PFCs, which are biologically inert molecules that have to be emulsified into lipid nanoemulsions[18] or incorporated into PLGA (poly(lactic-co-glycolic acid)) nanoparticles[19] for ^{19}F MRI (Figure 2). Untargeted PFCs are routinely injected 12-48h before the imaging session to ensure sufficient uptake, while targeted PFCs can be injected ~2h before imaging (here, PFCs still freely circulating will not generate a signal in TSE imaging, allowing only bound PFC to generate a signal). PFCs used in imaging are (1) small molecules (molecular weight <1,000Da)[20], (2) perfluorinated polymers[21] and (3) perfluorocarbon-hydrocarbon conjugates.[22] Nanoemulsions are oil-in-water colloidal dispersions, kinetically stabilized with a relatively low amount of surfactants (<10%) and a typical size below 500 nm, sufficiently small to pass through capillaries.[23,24] Theycan be produced by low-energy and high-energy methods,[25] and in some instances on an industrial scale.[26] PFCs are highly hydrophobic compounds with significant lipophobicity.[27] Because of this, PFCs require emulsification with surfactants through high energy homogenization, most commonly sonication or microfluidization, to yield stable PFC (nano)emulsions in water.[18]

The utility of PFCs for ^{19}F MRI is highly dependent on their chemical structure, which determines nanoemulsion formation, biological half-life, and retention in tissues.[20] Fluorescent dyes or targeting ligands can be incorporated into the PFC nanoemulsions by either insertion into the surfactant layer[28] or chemical conjugation,[29] to enable their selective detection in histological tissue samples or by flow cytometry.[21] Colloidal and fluorescence stability must be maintained

throughout the lifetime of nanoemulsion from the time of manufacturing through its storage and use. Robust mathematical modelling approaches were developed to better control nanoemulsions colloidal and fluorescence properties by customizing their composition and manufacturing processing parameters.[30] Furthermore, several approaches have been described to improve the relaxation times of the designed nanoemulsions by incorporating paramagnetic agents such as gadolinium or iron ions (Figure 2).[31–33] In practice, tracers are either produced in-house with well-established quality control procedures, acquired through collaborations, or bought from various small companies. For selective targeting approaches, the PFC surface has to be equipped with (i) poly-ethylene-glycol which generates a rejective force towards opsonization by serum proteins thereby impairing the uptake by phagocytic cells in the blood and (ii) reactive click-chemistry groups (e.g. maleimide) which enables the coupling of ligands to the surface of PFCs to generate specificity against certain epitopes.[34] Depending on the substance and the chemical environment, the range of chemical shifts of PFC tracers can vary over a very broad range of ~400 ppm (compared to ^{1}H with about 10 ppm).[35] This broad chemical shift range leads to an excellent separation of individual ^{19}F signals providing the base for multiplex and multitargeting approaches.[36,37]

Pulse sequence design

One of the main challenges in ^{19}F MRI is its relatively low sensitivity, since micro- to millimolar PFC concentrations need to be detected directly: for conventional ^{1}H MRI, we can work with ~50M of water in the human body. However, since the injected PFC is the only MRI-detectable compound, there is no need to optimize contrast between tissues, and the pulse sequence can be adapted to maximize signal. The optimal pulse sequence will strongly depend on the application: different magnetic field strengths, PFC formulations and investigated organs will have their own optimum. The T_1 relaxation times of PFCs typically used are relatively long (1-4s), which dictates several aspects of the choice of pulse sequence. It should be noted that no anatomical

10

markers are visualized ^{19}F MRI, so anatomical co-registration is achieved with the acquisition of

^{1}H and ^{19}F slices in the same orientation and field-of-view during the same session. In addition,

^{19}F MRI can easily be made fully quantitative by measuring the RF transmit/receive field and by

placing a reference tube with known PFC concentration within the image plane: since the

injected PFC is the only source of signal, the signal strength is directly proportional to the

concentration.

If a PFC with a single resonance is injected, a high-signal pulse sequences such as turbo spin

echo (TSE), balanced steady-state free precession (bSSFP) and ultrashort echo time (UTE)[38]

should be used to maximize precision. Each of these has advantages and disadvantages (TSE is

sensitive to motion, bSSFP is sensitive to magnetic field inhomogeneities, UTE uses an

insensitive readout, etc.), but they all have pulse sequence parameters that can be optimized as a

function of the T_1 and T_2 relaxation times of the PFC.[39] The usual MRI tradeoffs can also be

made: if a lower limit of detection (LoD) is desired, extra scan time can be invested and larger

pixel/voxel sizes can be used. It has recently been demonstrated that compressed sensing can be

combined with ^{19}F MRI to accelerate the acquisition and to denoise the images,[40] and thus to

increase precision[41] (Figure 3).

A common challenge in ^{19}F MRI physics arises when PFCs with multiple resonances (such as

perfluoro-octylbromide; PFOB) are imaged. Their magnetically non-equivalent fluorine atoms

have large differences in resonance frequencies and will generate chemical shift artifacts if these

are not corrected for (Figure 3B), but these PFCs are often preferred because of their fast

elimination from the body and thus higher likelihood to be approved by regulatory bodies.

Several methods have been proposed to overcome this challenge. Initially, these consisted of

linear deconvolution[42] (which results in noise amplification) and selective excitation[43,44] (skipping

part of the potential signal), but recently several solutions that excite all resonances with highly sensitive pulse sequences have been proposed. These include chemical shift encoding with bSSFP (similar to Dixon-like water-fat separation)[45], multi-chemical-shift-selective TSE (which selectively excites each resonance in turn during the recovery period)[12], and iterative deconvolution[46] (where the noise amplification is avoided).

While the large diversity of pulse sequences might initially appear overwhelming, there is now a tailored solution for nearly every application.

7. Demonstrated cardiovascular applications

Inflammation monitoring

The first comprehensive validation of ^{19}F MRI as a sensitive means to assess murine cardiac tissue inflammation *in vivo* was carried out in 2008.[47] Several years later, a similar approach was applied to a rat model of reperfused MI to visualize the spatiotemporal recruitment of monocytes *in vivo*.[16] However, it took almost one decade more for the principal feasibility of these small animal high field studies to be translated to a clinical setup by employing adult pigs subjected to ischemia-reperfusion injury.[8,48] Here, the co-localization of the ^{19}F signal with leukocytes and the quantitative relationship of this signal to the number of cells was demonstrated (Figure 4). Importantly, *in vivo* ^{19}F MRI identified inflammatory infiltration as independent determinant of LV contractile function and geometry early after AMI.[8]

Beyond AMI, ^{19}F MRI also proved to be suitable for monitoring cardiac inflammation in models of myocarditis and transplant rejection (Figure 5A-B). Of note, both autoimmune and viral myocarditis could reliably be identified after PFC application at independent sites.[49,50] Similarly, organ rejection was successfully visualized by different groups in both rats and mice with

excellent sensitivity and specificity.[51,52] [19]F MRI is also useful to detect inflammation in atherosclerotic plaques[53] (Fig. 5C), which was extended to demonstrate that this technique holds the potential for an early and sensitive prognosis of major cardiovascular events.[12] By tracking PFC-loaded immune cells, mice at risk for development of MI could be readily identified at a time point when no other parameter (neither functional scores nor LGE) was indicative (Fig. 5D). Furthermore, using a multicolor approach with three individual PFCs directed to inflammatory foci, early and mature thrombi, sites affected by low-grade inflammation, freshly developed and advanced pulmonary thrombi could be discriminated in one single scan (Fig. 5F left, top). Importantly, the early identification of these vulnerable spots was followed by massive right ventricular (RV) dilation und and functional impairment (Fig. 5F right). These findings demonstrate that multi-targeted PFCs allow the reliable identification of still silent but prognostically highly relevant thromboinflammation prior to any subsequent ischemic or thromboembolic event. By concurrent detection of several hallmarks of disease progression, it maps the entire transition from beginning coronary inflammation to microembolization, vessel occlusion and MI.[12]

Targeted imaging

Targeted PFCs can likewise be engineered with antibodies or binding peptides specifically directed against integrins expressed in angiogenesis[54] or cell populations such as neutrophils.[11] In the latter study, intravenous tracer injection prior to ischemia-reperfusion injury allowed the non-invasive 3D visualization of neutrophils within their different hematopoietic niches throughout the body and the subsequent monitoring of their egress into myocardium due the myocardial injury (Figure 6).

Cell tracking

While the approaches described in the previous sections all made use of an *in situ* labeling of the targets structures after intravenous PFC injections, *ex vivo* labeling strategies have also been used. Here the first step consists of isolating, characterizing, and expanding the cells to be tracked. Next, the cells are incubated with PFCs to "load" the cells and subsequently the ^{19}F-labeled cells are re-transplanted by either intravenous, intraperitoneal or subcutaneous injection. This approach has been successfully used to track the migration of ^{19}F-labeled T cells from the intraperitoneal injection site to the pancreas in a non-obese diabetic mouse model[55] and even in humans to detect immunotherapeutic dendritic cells delivered to colorectal adenocarcinoma patients.[56] However, in the cardiovascular field few applications have been reported, e.g. for detection of cardiac progenitor stem cells after intracardial injection (Figure S1).[57]

8. Clinical translation

While the medical need, technical possibilities, and pathophysiological applications of ^{19}F MRI are evident, several standing challenges for the translation of the technique to clinical exams exist (Figure 7). In short, for ^{19}F MRI to be added to a research program, three steps will need to be taken: 1) assuring that the MR scanner is capable of ^{19}F MRI (broadband amplifier, RF coil, and a pulse sequence) 2) obtaining a PFC tracer through production, collaboration, or purchase, and 3) obtaining regulatory approval.

Since the gyromagnetic ratio of ^{19}F is high, a clinically common magnetic field strength of 1.5 or 3T appears to be sufficient to achieve both high SNR and sensitivity in human applications of ^{19}F MRI. However, it should be noted that many clinical MRI systems will need relevant upgrades. These are typically available from the scanner manufacturers, while CE- or FDA-approved RF

coil designs are available from third-party vendors. Practical hardware costs to add ^{19}F MR capabilities to an existing scanner depend on a variety of factors such the country and existing contracts, but should be on the same order as the costs of replacing a regular amplifier or adding an RF coil.

As any molecule for routine medical use, PFCs need to pass through phase I toxicity and dose finding trials. Therefore, collaboration with industry may be important at this stage of development. Fortunately, several PFCs were originally of clinical interest as synthetic blood substitutes (i.e. volume expanders) as well as for liquid ventilation, so there is a large body of previous clinical trials that can potentially be leveraged to facilitate approval. Phase I and phase II clinical trials without a ^{19}F MRI indication were undertaken with PFOB (known then as Perflubron or Oxygent) and perfluorodecalin (marketed as Fluosol and Perftoran), several of which were FDA approved for several years, but discontinued by their manufacturers.[27] More recently, phase I and II trials have been initiated with perfluoro-tert-butylcyclohexane (PFTBH, known as Oxycyte or ABL-101), which also has a highly favorable MRI-profile.[58] Encouragingly, ^{19}F MRI was already used for cell tracking in a small clinical trial to detect immunotherapeutic dendritic cells delivered to colorectal adenocarcinoma patients.[56]

The tracer dosage needs to be scaled from mouse to man while taking both sensitivity and safety into account. For the purpose of imaging monocytes/macrophages with non-targeted nanoparticles on clinical scanners, a dose of 5mL/kg body weight has been safely and efficiently used in large animals to generate SNR of 10-30.[8] Even with the used single-element surface RF coil and standard image reconstruction, the injected PFC dose could have been reduced to track hot spots of inflammation in patients. The abovementioned dose (up to 400 mL) can likely be reduced more than ten-fold in clinical practice, when optimizing the PFC load per nanoparticle,[58]

taking the superior phagocytosis capacity of human cells into consideration,[59] and improving ^{19}F signal acquisition by using phased-array RF coils or adding combined compressed sensing and averaging.[41] As detailed in Table 1, the dose of 400ml already led to a five-fold higher sensitivity than clinical PET approaches. . This high sensitivity is further illustrated by the detection of small atherosclerotic inflammation loci in a mouse model on a clinical 3T scanner.[17]

9. Outlook

[19]F MRI is a unique cardiovascular imaging technique with several distinctive features that can be a decisive complement to other imaging modalities. In the preclinical setting, it has been used to elucidate a broad range of biological mechanisms as well as to quantify and monitor inflammation in several disease models. Continuous improvement in the hardware, pulse sequences, and tracer formulations ensures an exciting future for this field. Manufacturing of PFC formulations for clinical translation is made feasible through application of quality-by-design methodologies, which assures both scalability and final product quality.[60] The main current limitation of the technique is the lack of regulatory-approved tracers, necessitating further dose finding studies for specific medical indications.

The push from several directions for translation of ^{19}F MRI to a clinical application illustrates that the technique has matured sufficiently to make this leap. Clinical 3T scanners have been shown to allow for sufficient sensitivity to detect cardiovascular inflammation in both small and large animal models, and the latter was even shown to predictively correlate with remodeling. The regulatory approval of the tracer can likely be resolved either through using formulations that were previously approved for other applications (blood replacement, ventilation) or by working with a strong industrial partner that is interested in developing the market for a new

diagnostic modality. A combined therapeutic and diagnostic ("theranostic") approach might be the answer to the latter option, since PFCs have a therapeutic capacity to dissolve oxygen that is five times higher than blood and PFC nanoparticles are much smaller than erythrocytes, which has led to industry-driven clinical trials for tissue reoxygenation therapy after stroke and traumatic brain injury.[27]

In our opinion, the most feasible target for a first clinical trial is either 1) AMI, which has a high concentration of leukocytes as well as a direct link of the inflammation load to myocardial function, or 2) carotid atherosclerosis, where the inflamed plaque is close to the surface and can thus yield high signals, while a gold-standard comparison can be made through histology of the excised plaque after endarterectomy. A convincing clinical outcome in either would send a strong signal for the complementary diagnostic information that ^{19}F MRI provides and could open the doors for a range of follow-up studies.

10. References

1. Weissleder R, Elizondo G, Wittenberg J, Rabito CA, Bengele HH, Josephson L. Ultrasmall superparamagnetic iron oxide: characterization of a new class of contrast agents for MR imaging. *Radiology*. 1990;175:489–493.
2. Rieckmann M, Delgobo M, Gaal C, Büchner L, Steinau P, Reshef D, et al. Myocardial infarction triggers cardioprotective antigen-specific T helper cell responses. *J Clin Invest*. 2019;129:4922–4936.
3. Reiter T, Kircher M, Schirbel A, Werner RA, Kropf S, Ertl G, et al. Imaging of C-X-C Motif Chemokine Receptor CXCR4 Expression After Myocardial Infarction With [68Ga]Pentixafor-PET/CT in Correlation With Cardiac MRI. *JACC Cardiovasc Imaging*. 2018;11:1541–1543.
4. Heo GS, Bajpai G, Li W, Luehmann HP, Sultan DH, Dun H, et al. Targeted PET Imaging of Chemokine Receptor 2-Positive Monocytes and Macrophages in the Injured Heart. *J Nucl Med*. 2021;62:111–114.
5. Lapa C, Reiter T, Li X, Werner RA, Samnick S, Jahns R, et al. Imaging of myocardial inflammation with somatostatin receptor based PET/CT — A comparison to cardiac MRI. *Int J Cardiol*. 2015;194:44–49.
6. Fischer BM, Olsen MWB, Ley CD, Klausen TL, Mortensen J, Højgaard L, et al. How few cancer cells can be detected by positron emission tomography? A frequent question addressed by an in vitro study. *Eur J Nucl Med Mol Imaging*. 2006;33:697–702.

7. Holcman K, Rubiś P, Stępień A, Graczyk K, Podolec P, Kostkiewicz M. The Diagnostic Value of 99mTc-HMPAO-Labelled White Blood Cell Scintigraphy and 18F-FDG PET/CT in Cardiac Device-Related Infective Endocarditis—A Systematic Review. *J Pers Med*. 2021;11:1016.

8. Bönner F, Gastl M, Nienhaus F, Rothe M, Jahn A, Pfeiler S, et al. Regional analysis of inflammation and contractile function in reperfused acute myocardial infarction by in vivo 19F cardiovascular magnetic resonance in pigs. *Basic Res Cardiol*. 2022;117:21.

9. Pavon AG, Meier D, Samim D, Rotzinger DC, Fournier S, Marquis P, et al. First Documentation of Persistent SARS-Cov-2 Infection Presenting With Late Acute Severe Myocarditis. *Can J Cardiol*. 2020;36:1326.e5-1326.e7.

10. Bonaca MP, Olenchock BA, Salem J-E, Wiviott SD, Ederhy S, Cohen A, et al. Myocarditis in the Setting of Cancer Therapeutics: Proposed Case Definitions for Emerging Clinical Syndromes in Cardio-Oncology. *Circulation*. 2019;140:80–91.

11. Bouvain P, Ding Z, Kadir S, Kleimann P, Kluge N, Tiren Z-B, et al. Non-invasive mapping of systemic neutrophil dynamics upon cardiovascular injury. *Nat Cardiovasc Res*. 2023;2:126–143.

12. Flögel U, Temme S, Jacoby C, Oerther T, Keul P, Flocke V, et al. Multi-targeted 1H/19F MRI unmasks specific danger patterns for emerging cardiovascular disorders. *Nat Commun*. 2021;12:5847.

13. Ridker PM, Everett BM, Thuren T, MacFadyen JG, Chang WH, Ballantyne C, et al. Antiinflammatory Therapy with Canakinumab for Atherosclerotic Disease. *N Engl J Med*. 2017;377:1119–1131.

14. Fernández-Friera L, Fuster V, López-Melgar B, Oliva B, Sánchez-González J, Macías A, et al. Vascular Inflammation in Subclinical Atherosclerosis Detected by Hybrid PET/MRI. *J Am Coll Cardiol*. 2019;73:1371–1382.

15. Temme S, Grapentin C, Quast C, Jacoby C, Grandoch M, Ding Z, et al. Noninvasive Imaging of Early Venous Thrombosis by ^{19}F Magnetic Resonance Imaging With Targeted Perfluorocarbon Nanoemulsions. *Circulation*. 2015;131:1405–1414.

16. Ye Y-X, Basse-Lüsebrink TC, Arias-Loza P-A, Kocoski V, Kampf T, Gan Q, et al. Monitoring of monocyte recruitment in reperfused myocardial infarction with intramyocardial hemorrhage and microvascular obstruction by combined fluorine 19 and proton cardiac magnetic resonance imaging. *Circulation*. 2013;128:1878–1888.

17. Darçot E, Colotti R, Pellegrin M, Wilson A, Siegert S, Bouzourene K, et al. Towards Quantification of Inflammation in Atherosclerotic Plaque in the Clinic - Characterization and Optimization of Fluorine-19 MRI in Mice at 3 T. *Sci Rep*. 2019;9:17488.

18. Janjic JM, Shao P, Zhang S, Yang X, Patel SK, Bai M. Perfluorocarbon nanoemulsions with fluorescent, colloidal and magnetic properties. *Biomaterials*. 2014;35:4958–4968.

19. Srinivas M, Tel J, Schreibelt G, Bonetto F, Cruz L-J, Amiri H, et al. PLGA-encapsulated perfluorocarbon nanoparticles for simultaneous visualization of distinct cell populations by 19F MRI. *Nanomedicine (Lond)*. 2015;10:2339–2348.

20. Jacoby C, Temme S, Mayenfels F, Benoit N, Krafft MP, Schubert R, et al. Probing different perfluorocarbons for in vivo inflammation imaging by 19F MRI: image reconstruction, biological half-lives and sensitivity. *NMR Biomed*. 2014;27:261–71.

21. Janjic JM, Srinivas M, Kadayakkara DKK, Ahrens ET. Self-delivering nanoemulsions for dual fluorine-19 MRI and fluorescence detection. *J Am Chem Soc*. 2008;130:2832–2841.

22. Du W, Nyström AM, Zhang L, Powell KT, Li Y, Cheng C, et al. Amphiphilic hyperbranched fluoropolymers as nanoscopic 19F magnetic resonance imaging agent assemblies. *Biomacromolecules*. 2008;9:2826–2833.

23. McClements DJ. Nanoemulsions versus microemulsions: terminology, differences, and similarities. *Soft Matter*. 2012;8:1719–1729.
24. Kotta S, Khan AW, Pramod K, Ansari SH, Sharma RK, Ali J. Exploring oral nanoemulsions for bioavailability enhancement of poorly water-soluble drugs. *Expert Opin Drug Deliv*. 2012;9:585–598.
25. Tadros T, Izquierdo P, Esquena J, Solans C. Formation and stability of nano-emulsions. *Adv Colloid Interface Sci*. 2004;108–109:303–318.
26. Mitri K, Vauthier C, Huang N, Menas A, Ringard-Lefebvre C, Anselmi C, et al. Scale-up of nanoemulsion produced by emulsification and solvent diffusion. *J Pharm Sci*. 2012;101:4240–4247.
27. Krafft MP, Riess JG. Therapeutic oxygen delivery by perfluorocarbon-based colloids. *Adv Colloid Interface Sci*. 2021;294:102407.
28. Akers WJ, Zhang Z, Berezin M, Ye Y, Agee A, Guo K, et al. Targeting of alpha(nu)beta(3)-integrins expressed on tumor tissue and neovasculature using fluorescent small molecules and nanoparticles. *Nanomedicine (Lond)*. 2010;5:715–726.
29. Balducci A, Wen Y, Zhang Y, Helfer BM, Hitchens TK, Meng WS, et al. A novel probe for the non-invasive detection of tumor-associated inflammation. *Oncoimmunology*. 2013;2:e23034.
30. Herneisey M, Janjic JM. Multiple Linear Regression Predictive Modeling of Colloidal and Fluorescence Stability of Theranostic Perfluorocarbon Nanoemulsions. *Pharmaceutics*. 2023;15:1103.
31. Neubauer AM, Myerson J, Caruthers SD, Hockett FD, Winter PM, Chen J, et al. Gadolinium-modulated 19F signals from perfluorocarbon nanoparticles as a new strategy for molecular imaging. *Magn Reson Med*. 2008;60:1066–1072.
32. Kislukhin AA, Xu H, Adams SR, Narsinh KH, Tsien RY, Ahrens ET. Paramagnetic fluorinated nanoemulsions for sensitive cellular fluorine-19 magnetic resonance imaging. *Nature Mater*. 2016;15:662–668.
33. Perez AS, Zhou J, Leach B, Xu H, Lister D, Adams SR, et al. Click-Ready Perfluorocarbon Nanoemulsion for ^{19}F MRI and Multimodal Cellular Detection. *ACS Nanosci Au*. 2022;2:102–110.
34. Bouvain P, Temme S, Flögel U. Hot spot 19 F magnetic resonance imaging of inflammation. *Wiley Interdiscip Rev Nanomed Nanobiotechnol*. 2020;12:e1639.
35. Ruiz-Cabello J, Barnett BP, Bottomley PA, Bulte JW. Fluorine (19F) MRS and MRI in biomedicine. *NMR Biomed*. 2011;24:114–29.
36. Akazawa K, Sugihara F, Nakamura T, Matsushita H, Mukai H, Akimoto R, et al. Perfluorocarbon-Based 19 F MRI Nanoprobes for In Vivo Multicolor Imaging. *Angew Chem Int Ed Engl*. 2018;57:16742–16747.
37. Cohen D, Mashiach R, Houben L, Galisova A, Addadi Y, Kain D, et al. Glyconanofluorides as Immunotracers with a Tunable Core Composition for Sensitive Hotspot Magnetic Resonance Imaging of Inflammatory Activity. *ACS nano*. 2021;15:7563–7574.
38. Goette MJ, Keupp J, Rahmer J, Lanza GM, Wickline SA, Caruthers SD. Balanced UTE-SSFP for 19F MR imaging of complex spectra. *Magn Reson Med*. 2015;74:537–43.
39. Mastropietro A, De Bernardi E, Breschi GL, Zucca I, Cametti M, Soffientini CD, et al. Optimization of rapid acquisition with relaxation enhancement (RARE) pulse sequence parameters for ^{19}F-MRI studies. *J Magn Reson Imaging*. 2014;40:162–170.
40. Zhong J, Mills PH, Hitchens TK, Ahrens ET. Accelerated fluorine-19 MRI cell tracking using compressed sensing. *Magn Reson Med*. 2013;69:1683–90.

41. Darçot E, Yerly J, Hilbert T, Colotti R, Najdenovska E, Kober T, et al. Compressed sensing with signal averaging for improved sensitivity and motion artifact reduction in fluorine-19 MRI. *NMR Biomed*. 2021;34:e4418.

42. Busse LJ, Thomas SR, Pratt RG, Clark Jr. LC, Ackerman JL, Samaratunga RC, et al. Deconvolution techniques for removing the effects of chemical shift in 19F nuclear magnetic resonance imaging of perfluorocarbon compounds. *Medical Physics*. 1986;13:518–524.

43. Giraudeau C, Flament J, Marty B, Boumezbeur F, Meriaux S, Robic C, et al. A new paradigm for high-sensitivity 19F magnetic resonance imaging of perfluorooctylbromide. *Magn Reson Med*. 2010;63:1119–24.

44. Laukemper-Ostendorf S, Scholz A, Bürger K, Heussel CP, Schmittner M, Weiler N, et al. 19F-MRI of perflubron for measurement of oxygen partial pressure in porcine lungs during partial liquid ventilation. *Magn Reson Med*. 2002;47:82–89.

45. van Heeswijk RB, Colotti R, Darçot E, Delacoste J, Pellegrin M, Piccini D, et al. Chemical shift encoding (CSE) for sensitive fluorine-19 MRI of perfluorocarbons with complex spectra. *Magn Reson Med*. 2018;79:2724–2730.

46. Schoormans J, Calcagno C, Daal MRR, Wüst RCI, Faries C, Maier A, et al. An iterative sparse deconvolution method for simultaneous multicolor 19F-MRI of multiple contrast agents. *Magn Reson Med*. 2020;83:228–239.

47. Flögel U, Ding Z, Hardung H, Jander S, Reichmann G, Jacoby C, et al. In vivo monitoring of inflammation after cardiac and cerebral ischemia by fluorine magnetic resonance imaging. *Circulation*. 2008;118:140–148.

48. Rothe M, Jahn A, Weiss K, Hwang J-H, Szendroedi J, Kelm M, et al. In vivo 19F MR inflammation imaging after myocardial infarction in a large animal model at 3 T. *Magn Reson Mater Phy*. 2019;32:5–13.

49. van Heeswijk RB, De Blois J, Kania G, Gonzales C, Blyszczuk P, Stuber M, et al. Selective in vivo visualization of immune-cell infiltration in a mouse model of autoimmune myocarditis by fluorine-19 cardiac magnetic resonance. *Circ Cardiovasc Imaging*. 2013;6:277–84.

50. Jacoby C, Borg N, Heusch P, Sauter M, Bonner F, Kandolf R, et al. Visualization of immune cell infiltration in experimental viral myocarditis by (19)F MRI in vivo. *Magma*. 2014;27:101–6.

51. Hitchens TK, Ye Q, Eytan DF, Janjic JM, Ahrens ET, Ho C. 19F MRI detection of acute allograft rejection with in vivo perfluorocarbon labeling of immune cells. *Magn Reson Med*. 2011;65:1144–53.

52. Flogel U, Su S, Kreideweiss I, Ding Z, Galbarz L, Fu J, et al. Noninvasive detection of graft rejection by in vivo (19) F MRI in the early stage. *Am J Transplant*. 2011;11:235–44.

53. van Heeswijk RB, Pellegrin M, Flögel U, Gonzales C, Aubert J-F, Mazzolai L, et al. Fluorine MR imaging of inflammation in atherosclerotic plaque in vivo. *Radiology*. 2015;275:421–429.

54. Winter PM, Morawski AM, Caruthers SD, Fuhrhop RW, Zhang H, Williams TA, et al. Molecular imaging of angiogenesis in early-stage atherosclerosis with alpha(v)beta3-integrin-targeted nanoparticles. *Circulation*. 2003;108:2270–2274.

55. Srinivas M, Morel PA, Ernst LA, Laidlaw DH, Ahrens ET. Fluorine-19 MRI for visualization and quantification of cell migration in a diabetes model. *Magn Reson Med*. 2007;58:725–734.

56. Ahrens ET, Helfer BM, O'Hanlon CF, Schirda C. Clinical cell therapy imaging using a perfluorocarbon tracer and fluorine-19 MRI. *Magn Reson Med*. 2014;72:1696–701.

57. Gonzales C, Yoshihara HAI, Van Heeswijk RB, Mieville P, Helm L, Blyszczuk P, et al. 19F-Magnetic Resonance Imaging for Tracking Bone-Marrow Macrophages in a Model of Experimental Autoimmune Myocarditis: A Pilot Study. *Biomed J Sci Tech Res*. 2020;29.

58. Darçot E, Colotti R, Brennan D, Deuchar GA, Santosh C, Heeswijk RB. A characterization of ABL-101 as a potential tracer for clinical fluorine-19 MRI. *NMR Biomed*. 2020;33:e4212.

59. Nienhaus F, Colley D, Jahn A, Pfeiler S, Flocke V, Temme S, et al. Phagocytosis of a PFOB-Nanoemulsion for 19F Magnetic Resonance Imaging: First Results in Monocytes of Patients with Stable Coronary Artery Disease and ST-Elevation Myocardial Infarction. *Molecules*. 2019;24:2058.

60. Herneisey M, Liu L, Lambert E, Schmitz N, Loftus S, Janjic JM. Development of Theranostic Perfluorocarbon Nanoemulsions as a Model Non-Opioid Pain Nanomedicine Using a Quality by Design (QbD) Approach. *AAPS PharmSciTech*. 2019;20:65.

11. Tables

Table 1. A comparison between several cardiovascular molecular imaging modalities. FDG probes transmembrane glucose transport in leukocytes, which also occurs in cardiomyocytes, thus limiting its specificity. The comparable cellular sensitivity of ^{19}F MRI is likely achieved with a significantly larger compound load than ^{18}FDG-PET.

	conventional ^{1}H-MRI	^{19}F MRI	^{18}FDG-PET	WBC-SPECT[7]
Existing pre-clinical evidence	yes	yes	yes	yes
Existing clinical evidence	yes	no	yes	limited
GMP/FDA approval	yes	no	yes	yes
Specificity	moderate	high	moderate	high

Sensitivity
 	
Cells per voxel at a given:
  - spatial resolution
  - acquisition duration
  - signal-to-noise ratio
	low	Bönner et al.[8]
		~2×10^6
		3$_x$3$_x$3mm^3
		20 min
		~20
			Fischer et al.[6]
			~10×10^6
			5$_x$5$_x$5mm^3
			5 min
			~20
				?

No background signal	no	yes	no	yes
No patient dietary preparation	yes	yes	no	no
No ionizing radiation	yes	yes	no	no

No other side effects (than radiation)	Possible	?	yes	yes

12.   Figures
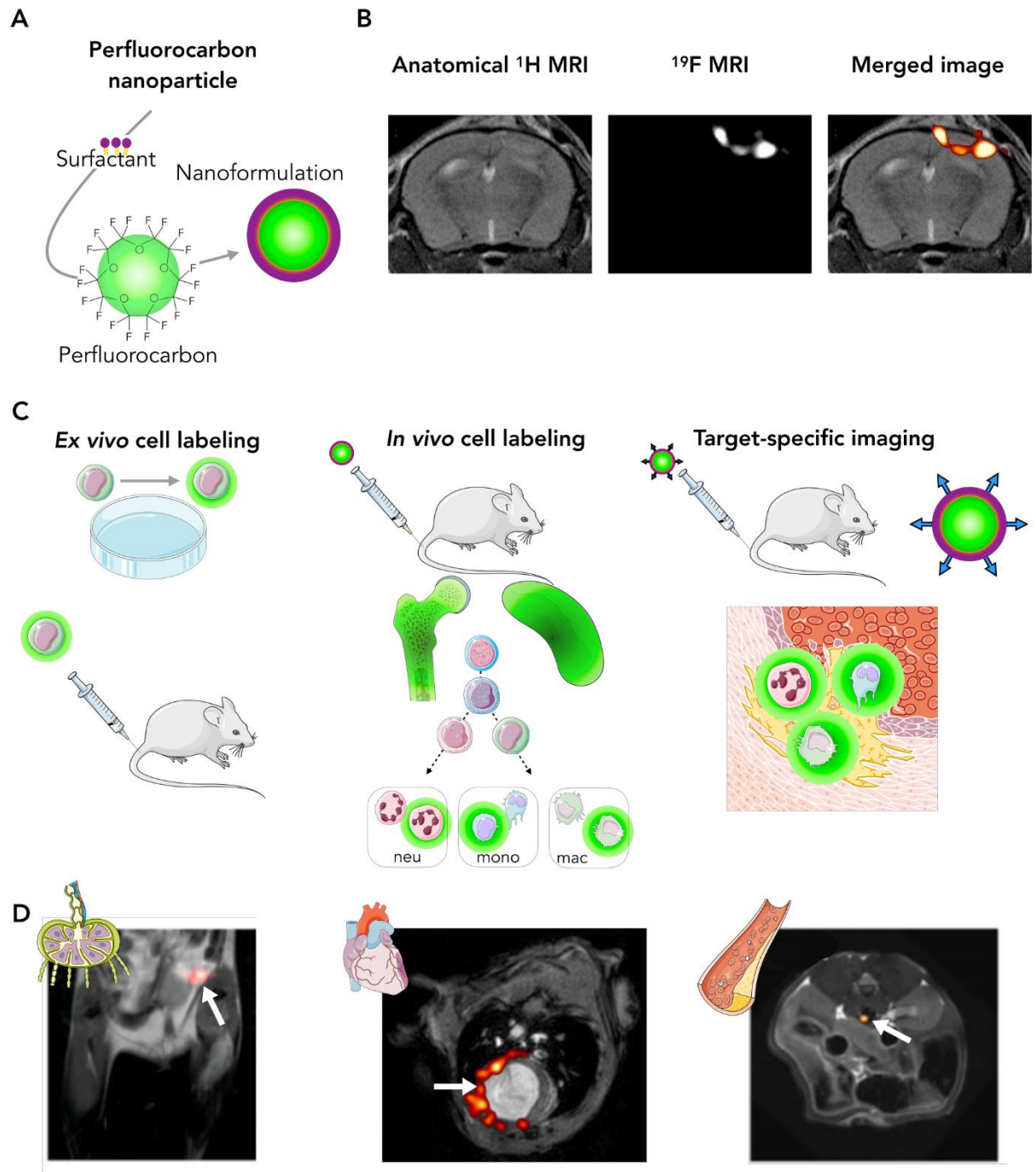
Figure 1. The principles and applications of ¹⁹F MRI. A) Lipophobic perfluorocarbon

molecules are packed in tracer nanoparticles. **B)** ¹⁹F MR images can be merged with ¹H reference

images for anatomical colocalization. **C)** Perfluorocarbon tracers can be used for ex-vivo cell labeling, in vivo cell labeling (such as inflammation imaging), or target specific imaging. **D)** Examples of these strategies include tracking the fate of specific cell populations as they enter lymph nodes (left), quantifying the inflammation burden after a myocardial infarction (middle) or visualizing the exact location of a thrombus (right).
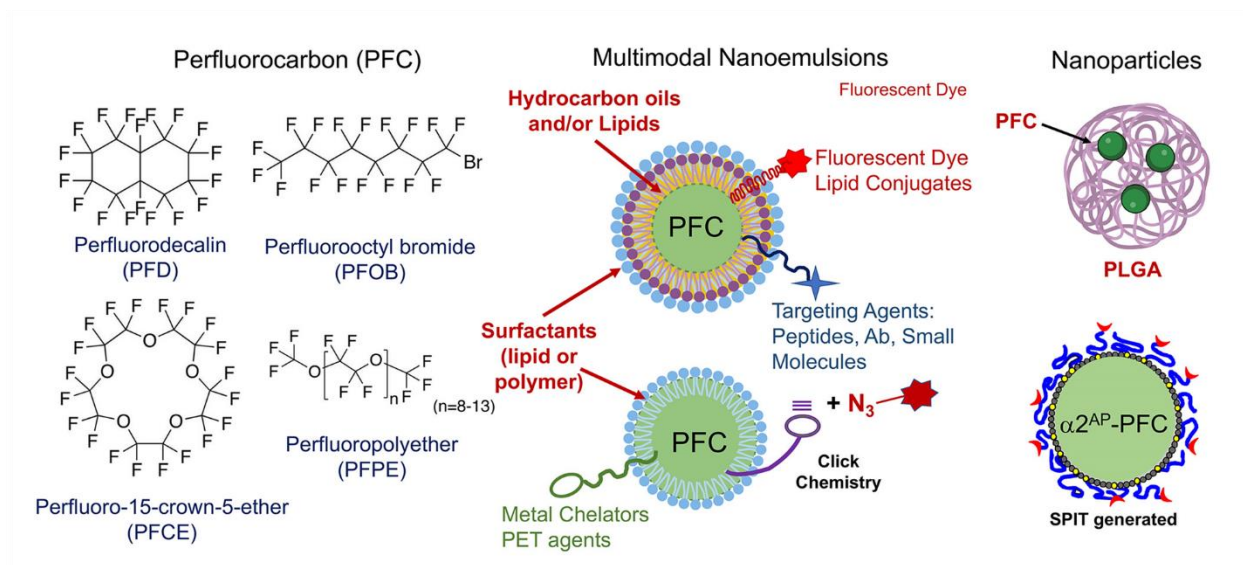
Figure 2. Structures of small molecule perfluorocarbons used for cell tracking by ^{19}F MRI. PFCs can be formulated as one of the two types of nanoemulsions: systems with a polymer or surfactant stabilizing the PFC oil droplets in aqueous media (bottom), or triphasic systems where the internal phase includes both PFCs and hydrocarbon, stabilized by a mixture of both lipid and polymeric surfactants[18] (top). Perfluorocarbons and surfactants can be further conjugated to targeting agents (e.g. fibrin[12]) and other moieties (e.g. fluorescent dyes[21], metal ion chelators[33]). Alternatively, PLGA particles can be doped with PFC oil droplets.[19]
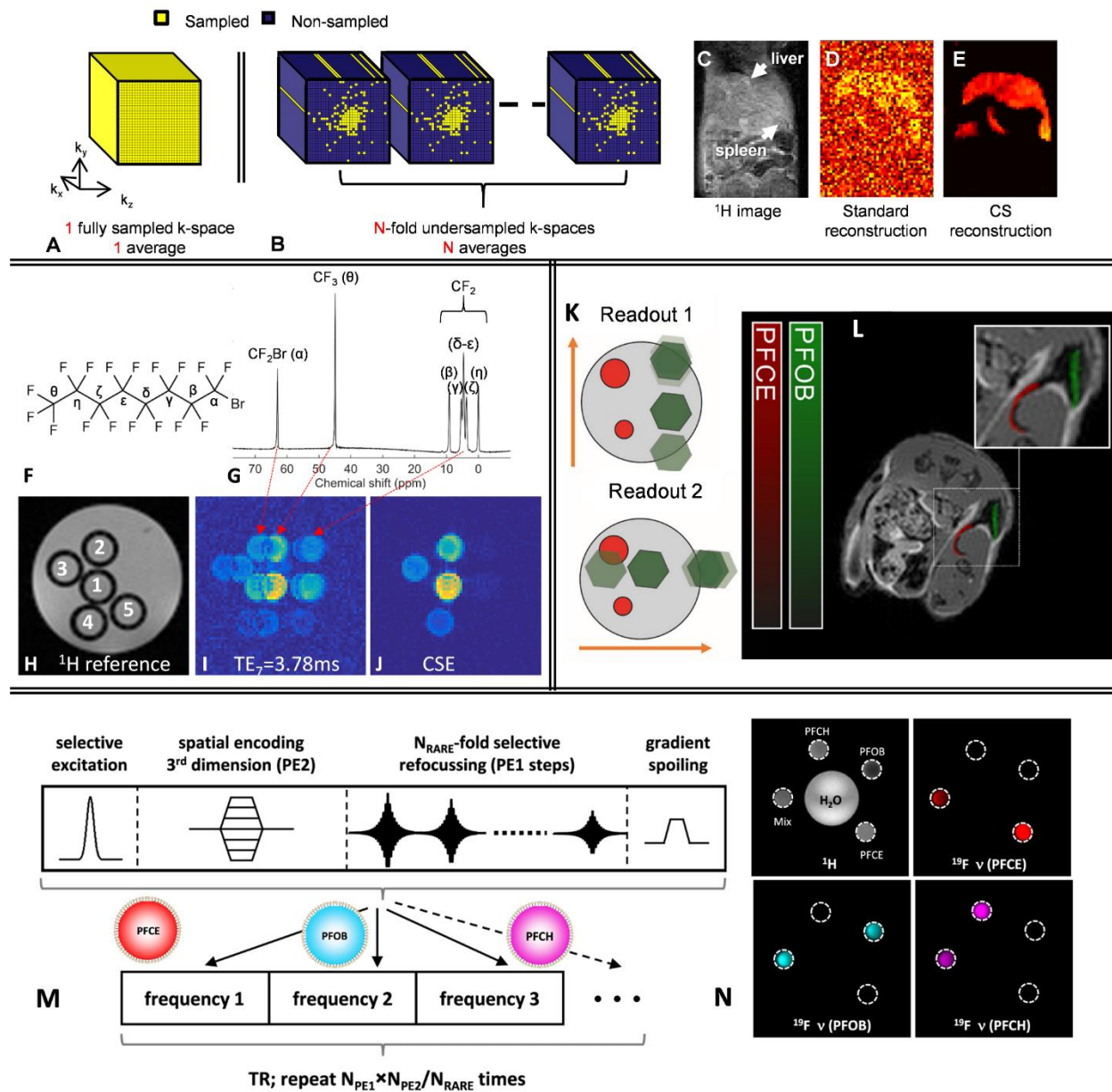
Figure 3. **MR pulse sequences developed to counter low signal and multiple signal-generating compounds. A-E)** Compressed sensing reconstruction can be combined with undersampling and averaging to increase the precision and motion robustness of ^{19}F MRI (adapted from Darçot et al.[41] with permission). **F-J)** Chemical shift encoding uses a range of echo times to remove chemical shift artifacts from compounds with multiple resonances (adapted from van Heeswijk et al.[45] with permission). **K-L)** Multiple resonances can also be untangled by

combining two different phase encoding directions with iterative reconstruction and

deconvolution (adapted from Schoormans et al.[46] with permission). **M)** The waiting time in a

frequency-selective 3D TSE pulse sequence can be used to encode different resonances. **N)** This

then allows multiple compounds to be resolved (adapted from Flögel et al.[12] with permission).

A

^{19}F CMR   Histology

in vivo   *ex vivo*   Infarct   Macrophages

CD68
CD163
DAPI

B

CMR: *In vivo* ^{19}F SNR

Histology: Macrophages [$\times 10^5$/mm^3]

$R^2 > 0.6075$
p<0.0001

C

^{19}F Integral [SNR·ml]

Enddiastolic Volume Index [ml/kg]

$R^2 > 0.6932$
p<0.0029
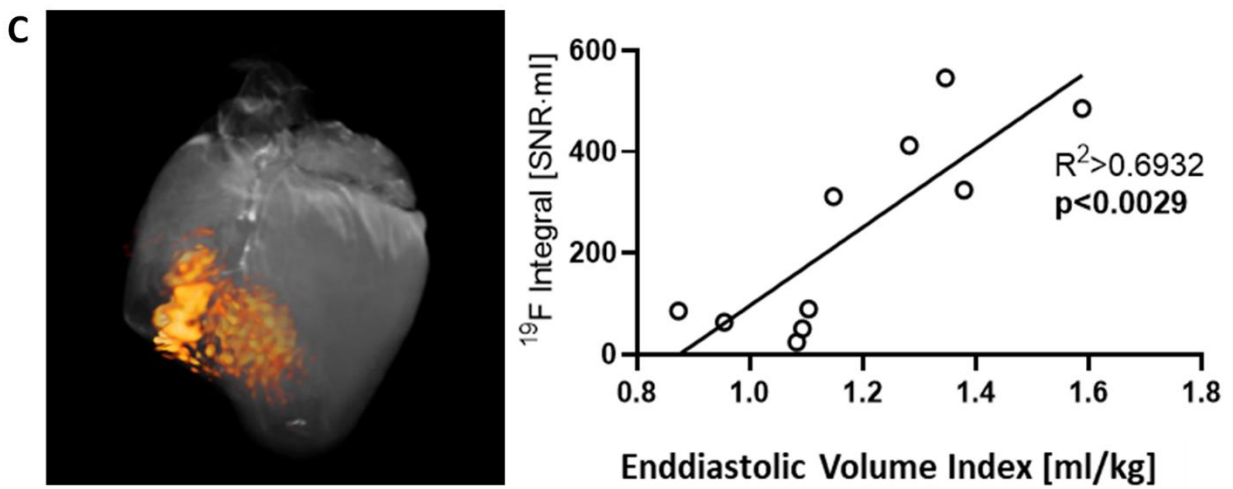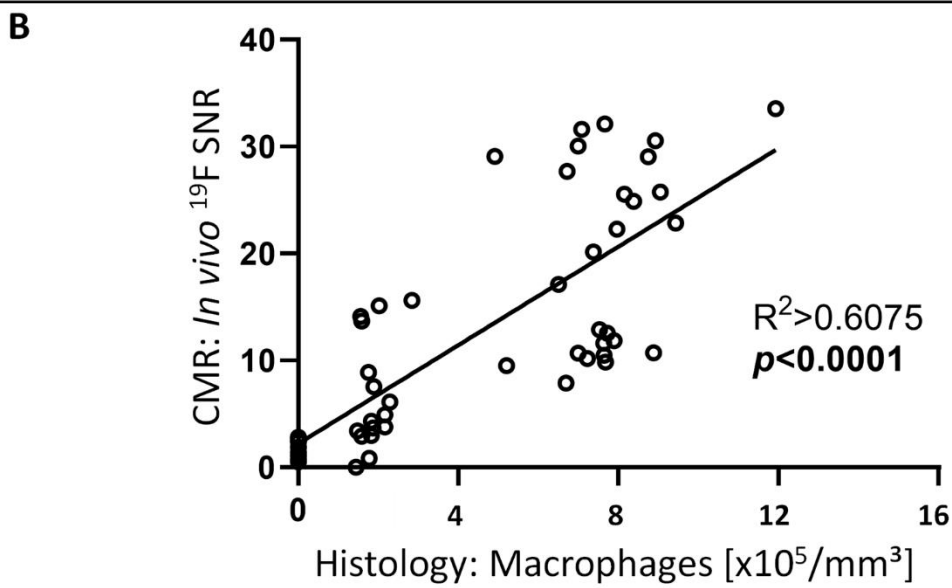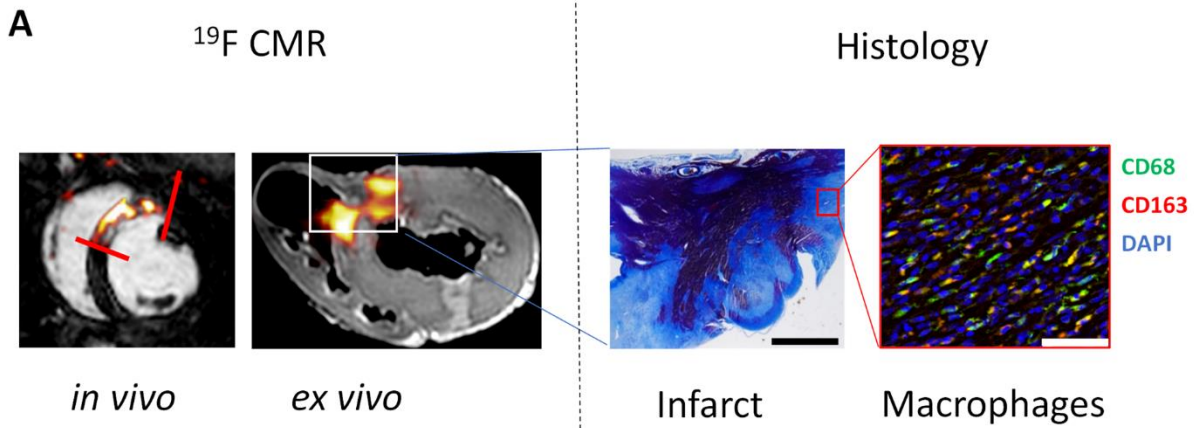
Figure 4. *In vivo* ^{19}**F CMR in a AMI pig model reflects macrophage density and myocardial remodeling. A)** Left: ^{19}F-signals are heterogeneously distributed in the area of infarction as observed *in vivo* (red lines) and *ex vivo* (white box). Right: Masson's trichrome stain with infarcted tissue (purple) and granulation tissue (blue), fluorescent staining with anti-macrophage antibodies (CD68 and CD163) and cellular nuclei (DAPI). Scale bar 50 µm. **B)** *In vivo* ^{19}F SNR plotted against histological macrophage density expressed as cells/mm^3. **C)** Whole-heart analysis of the ^{19}F integral is significantly correlated with left ventricular end-diastolic volume index (LVEDV). Adapted from Bönner et al.[8] with permission.
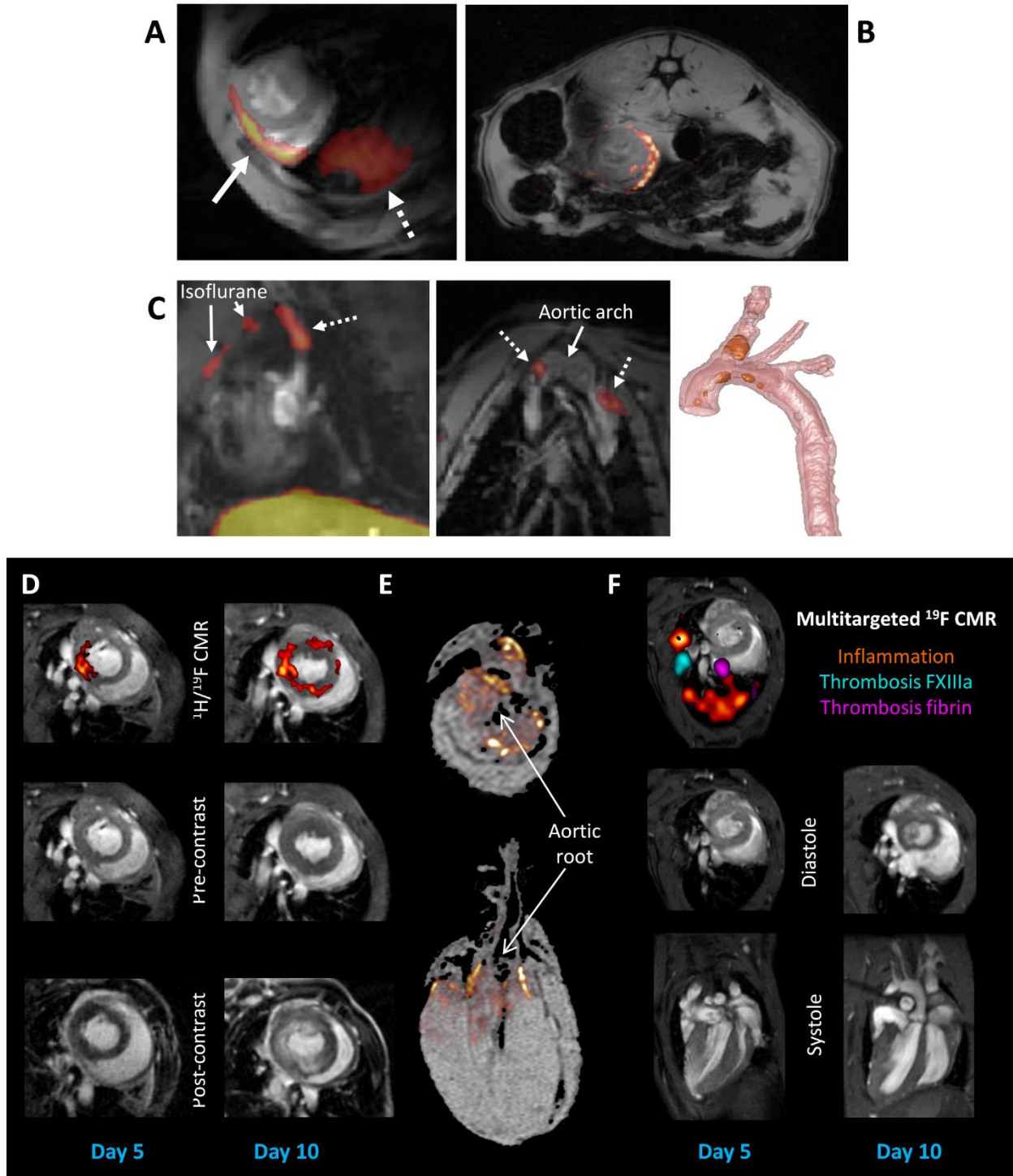
Figure 5. ^{19}F MRI applied to cardiovascular disease models. A) In a mouse model of autoimmune myocarditis, the ^{19}F signal colocalizes with the subepicardial layer of the LV anterior wall, the RV free wall (arrow) and the liver (dotted arrow). **B)** Fused *in vivo* ^{19}F and ^{1}H

MR images show the detection of PFC-labeled immune cells in the myocardium of a transplanted heart graft. **C)** Left: Sagittal ^{19}F/^{1}H fusion visualization of an atherosclerotic plaque (dotted arrow) as confirmed by histology. ^{19}F signals are also detected in liver and in the subcutaneous fat (uptake of the anesthetic isoflurane). Middle: Two plaques in the aortic arch are shown in another animal in a ^{19}F/^{1}H fusion image. Right: *Ex-vivo* high-resolution 3D rendering of an aorta and its ^{19}F signal. Inner and outer surface of the aortic wall are visualized in transparent pink, while the ^{19}F signal in orange can be seen to be located on the inner surface of the aortic arch and the brachiocephalic artery. **D-F)** Examples for prediction of MACE by longitudinal ^{1}H/^{19}F MRI acquired from the same animal at day 5 and 10 after onset of a high-fat diet. **D)** Tracking of PFC-loaded immune cells early revealed myocardial tissue (left, top) later prone to myocardial ischemia (right, bottom). **E)** *Post mortem* 3D ^{1}H/^{19}F MRI of **D** at an isotropic resolution of 40 μm. **F)** Multi-targeted, multi-color ^{19}F MRI for detecting inflammation (red; neat PFCs), freshly developed (cyan; α2-antiplasmin-targeted PFCs) and chronic (magenta; fibrin-targeted PFCs) thrombosis indicating differentially affected tissue sites leading finally to severe right ventricular impairment. Adapted with permission from van Heeswijk et al.,[49] Hitchens et al.,[51] van Heeswijk et al.,[53] and Flögel et al.,[12] respectively.
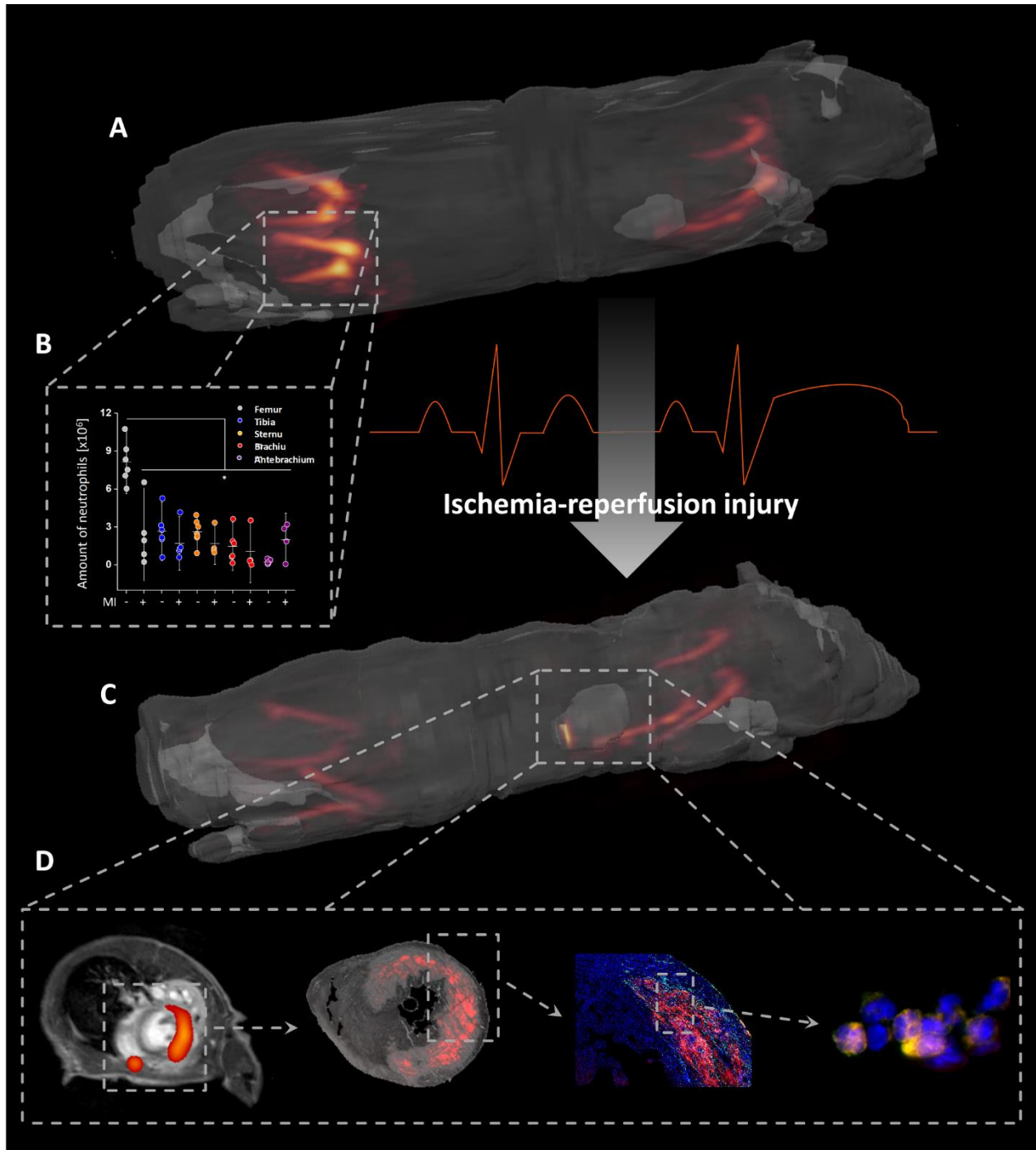
Figure 6. Mapping the trafficking of murine neutrophils after myocardial infarction. **A)** 3D whole-body ^{1}H/^{19}F MRI (grey/red) shows *in situ* labeling of neutrophils within their hematopoietic niches after injection of targeted PFCs. **B)** Flow-cytometric analysis of neutrophils in the different bone marrow compartments. **C)** Re-investigation 24 hrs post MI reveals

pronounced reduction of ^{19}F signals in the bone marrow of femur/tibia with simultaneous appearance of ^{19}F signal in the infarcted heart. **D)** Focal ^{1}H/^{19}F MRI (left) and subsequent histology confirms specific detection of rhodamine-labelled targeted PFCs within neutrophils (Ly6G-stained; right) infiltrated into the infarcted heart. Adapted from Bouvain et al.[11] with permission.
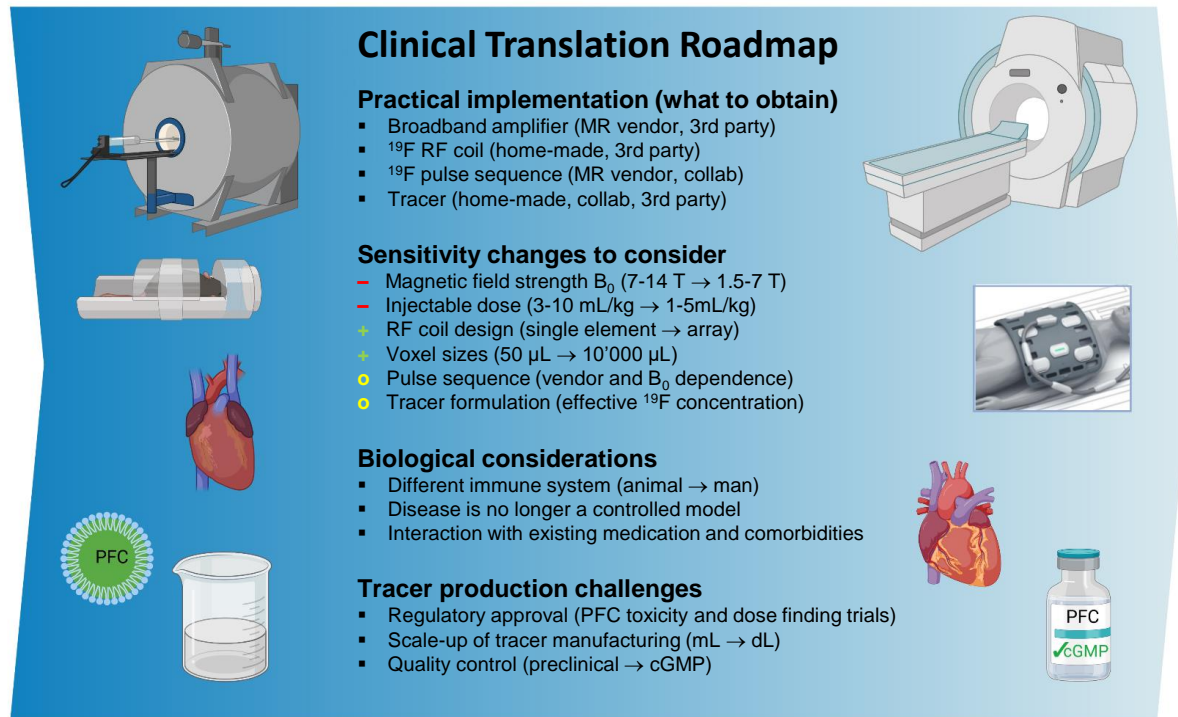
Figure 7. A roadmap for a successful translation of ^{19}F MRI to a clinical diagnostic modality. The practical implementation of ^{19}F MRI into an existing research program is straightforward and can mostly be effected straight away when taking expected sensitivity and biological changes into account. The production of a tracer with regulatory approval is the main remaining challenge.

13. Acknowledgments

14. Sources of Funding

15. Disclosures

16. Supplementary Material

Figure S1